JACS
JOURNAL OF THE AMERICAN CHEMICAL SOCIETY

Article

pubs.acs.org/JACS

Structure and Biosynthetic Assembly of Cupriachelin, a Photoreactive Siderophore from the Bioplastic Producer *Cupriavidus necator* H16

Martin F. Kreutzer, Hirokazu Kage, and Markus Nett*

Junior Research Group "Secondary Metabolism of Predatory Bacteria", Leibniz Institute for Natural Product Research and Infection Biology e.V., Hans-Knöll-Institute, Beutenbergstrasse 11a, 07745 Jena, Germany

Supporting Information

ABSTRACT: The bacterium *Cupriavidus necator* H16 produces a family of linear lipopeptides when grown under low iron conditions. The structural composition of these molecules, exemplified by the main metabolite cupriachelin, is reminiscent of siderophores that are excreted by marine bacteria. Comparable to marine siderophores, the ferric form of cupriachelin exhibits photoreactive properties. Exposure to UV light induces an oxidation of its peptidic backbone and a concomitant reduction of the coordinated Fe(III). Here, we report the genomics-inspired isolation and structural characterization of cupriachelin as well as its encoding gene cluster, which was identified by insertional mutagenesis. Based upon the functional characterization of adenylation domain specificity, a model for cupriachelin biosynthesis is proposed.

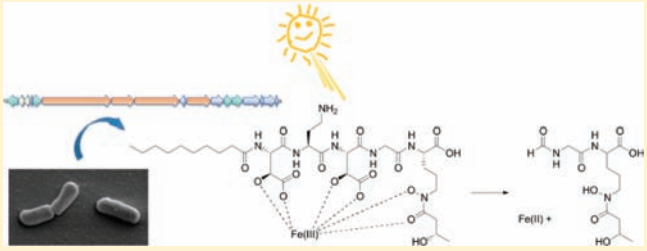

INTRODUCTION

Iron is indispensable for the vast majority of organisms due to its involvement in cellular respiration and metabolic processes.[1] Notwithstanding its abundance in the Earth's crust, the transition metal is not readily available in aerobic environments, including soil, freshwater, and marine habitats. At physiological pH and in the presence of water the biologically accessible form of the element, Fe(II), spontaneously oxidizes to give insoluble ferric oxide hydrate complexes. In order to overcome the environmental scarcity of ferrous iron, bacteria and fungi have thus evolved specific iron uptake systems.[1] One strategy involves the secretion of low molecular weight compounds, so-called siderophores, that coordinate Fe(III) with high affinity. Once a siderophore ligand has bound the metal ion, it is actively transported back into the cell, where the iron is released by a reductive (or hydrolytic) mechanism.[2] It has been shown that siderophore production may exert significant biological effects on the environment of an organism, be it the shaping of microbial communities[3] or the suppression of host defense mechanisms in case of a pathogenic siderophore producer.[4] Therefore, there is continued interest in the identification and functional characterization of these metabolites.

Genome mining approaches have proven to be particularly useful for the discovery of novel siderophores, as the high metal affinity of such compounds is associated with structural features that can be predicted by sequence analyses from their respective gene clusters; examples include catecholate or hydroxamate groups, which are commonly found in siderophores.[2] The assembly of these moieties typically requires a select set of biosynthetic genes,[5,6] and physical proximity to open reading frames encoding lipoprotein receptors and ABC-type iron transporters often provides ample evidence for the presence of a siderophore locus. The linkage of the different building blocks in siderophore biosynthesis is catalyzed by two distinct enzyme classes, namely nonribosomal peptide synthetases (NRPS)[7] and NRPS-independent siderophore synthetases (NIS).[8] Exploiting the inherent modular logic of the former,[9] it is possible to predict the structure of the encoded siderophore and to design selective protocols for its isolation. The first siderophore to be discovered applying an in silico strategy was coelichelin from the model actinomycete *Streptomyces coelicolor* A3(2) in 2005.[10] Since then, further previously unrecognized siderophores have been identified by genome mining approaches.[11−14] Notably, all these studies focused on actinobacteria, which are well-known for their secondary metabolic proficiency,[15] including siderophore biosynthesis, but not on other groups of microorganisms. This is surprising considering the increasing availability of microbial genome sequence data and the ensuing identification of neglected organisms as alternative natural product resources.[16]

In the present study, we investigated the potential of the industrially relevant bacterium *Cupriavidus necator* H16 (syn. *Ralstonia eutropha* H16) for siderophore biosynthesis. *C. necator* H16 is known to accumulate organic carbon in the form of polyhydroxyalkanoates, which have found wide application as raw materials for the production of medical devices.[17] Furthermore, the oxygen-tolerant [NiFe]-hydrogenases of the

Received: January 19, 2012
Published: March 1, 2012

   dx.doi.org/10.1021/ja300620z | *J. Am. Chem. Soc.* 2012, 134, 5415−5422

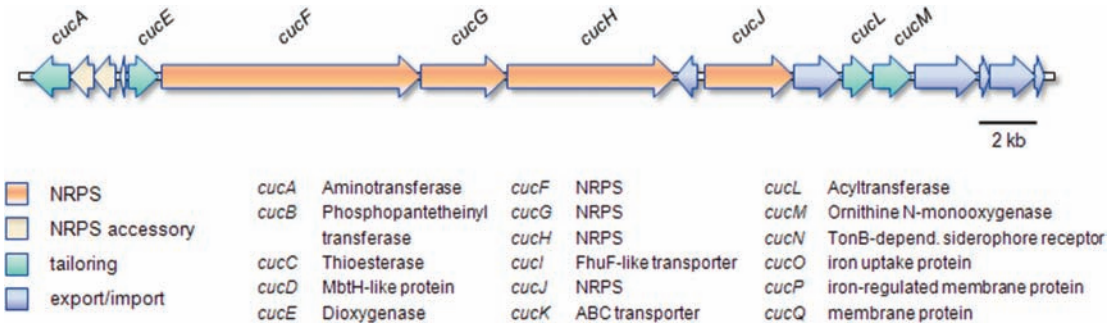

Figure 1. Organization of the *cuc* biosynthetic gene cluster. Genes are color-coded according to their proposed functions.

bacterium have attracted much interest, as they may serve as catalysts in photoelectrochemical biofuel cells.[18] In contrast, virtually nothing is known about the secondary metabolism of *C. necator* H16. Analysis of its genome sequence revealed the presence of a locus putatively involved in the biosynthesis of the siderophore vibrioferrin[19] as well as a chromosomally encoded NRPS gene cluster of unknown function.[20] The latter appears to be unique to the strain H16, lacking homologues even in phylogenetically related bacteria. The gene architecture of the orphan NRPS locus suggested a role in siderophore biosynthesis; a functional link with the annotated vibrioferrin-like cluster could not be excluded. Using a genome mining strategy that involved targeted gene disruption and comparative metabolic profiling of mutant and wild-type strains, we tracked the metabolites that derive from the NRPS gene cluster. The structure of the predominating compound, cupriachelin, was fully characterized by spectroscopic methods, and its stereochemistry was solved following chemical derivatization. Cupriachelin is unique in that it possesses characteristic physicochemical properties of marine siderophores, albeit the natural product is made by a terrestrial bacterium. The origin of the β-hydroxyaspartate moieties, which contribute to the photoreactivity of ferric cupriachelin, was biochemically interrogated.

RESULTS AND DISCUSSION

Architecture and Features of the NRPS Gene Cluster of Strain H16. A putative siderophore locus was identified on chromosome 2 of the *C. necator* H16 genome due to the local concentration of genes associated with iron-siderophore transport as well as siderophore assembly. Cluster boundaries were assigned on the basis of functional annotations, on the one hand, and operon predictions, on the other.[21] According to these analyses, the proposed cluster includes 17 ORFs between h16_B1676 and h16_B1692 covering 36.4 kb of contiguous DNA (Figure 1); the genes have been renamed in this study from *cucA* to *cucQ*.

A total of six genes (*cucI*, *cucK*, *cucN*, *cucO*, *cucP*, and *cucQ*) are involved in siderophore export and uptake, while four additional genes (*cucA*, *cucE*, *cucL*, and *cucM*) have likely roles in tailoring reactions. The latter two, *cucM* and *cucL*, were annotated to encode a lysine/ornithine N-monooxygenase and an acyltransferase, respectively. The concerted action of both enzymes would provide a hydroxamate moiety via an intermediary hydroxylamine group, analogous to other siderophore biosynthetic pathways.[8] In contrast, the functions of the putative aminotransferase CucA and of the dioxygenase CucE were less obvious. Among the seven remaining proteins encoded on the gene cluster, CucB represents a phosphopantetheinyl transferase and is thus essential to convert carrier protein domains in NRPSs from their *apo* into the active *holo* forms.[7] A similar role is conceivable for the MbtH-like protein CucD, which might contribute to the activation of amino acid building blocks as a cofactor.[22] The four NRPSs that derive from *cucF*, *cucG*, *cucH*, and *cucJ* are of particular interest, as they account for the peptidic backbone of the encoded metabolite. The corresponding proteins harbor five modules, each including the complete set of condensation (C), adenylation (A) and peptidyl carrier protein (PCP) domains, but they lack a typical loading module and a terminal thioesterase (TE) domain. While the offload from the assembly line might be accomplished by the discrete hydrolase CucC, no possible candidate gene for the activation of a starter unit was found within the cluster. The fact that all NRPSs include an N-terminal C domain is reminiscent, to a degree, to a situation known from the biosynthesis of lipopeptide antibiotics, in which a starter C domain acylates the first amino acid with a fatty acid.[23] To identify the substrates of the A domains in every NRPS module, we analyzed their putative binding pockets both manually and using computational specificity predictions.[24,25] Clear results were obtained only for three out of the five A domains (Table 1). The failure to predict substrate preferences for the second A domain in CucF and for the A domain of CucH hence suggested the priming of uncommon building blocks.

Table 1. Substrate Specificity Predictions for the Adenylation Domains of the NRPSs Encoded in the *cuc* Gene Cluster

A domain	signature sequence	substrate according to prediction
CucF-A_1	DLTKVGHVGK	L-Asp
CucF-A_2	DIWELTADDK	unknown
CucG	DLTKIGHIGK	L-Asp
CucH	DGEGSGGVTK	unknown
CucJ	DILQLGVVWK	Gly

A complete overview of the organization of the *cuc* gene cluster is provided in Table S1, Supporting Information.

Discovery and Isolation of Cupriachelin. We first noted the secretion of iron-chelating metabolites by *C. necator* H16 in the modified chrome azurol S (CAS) agar assay, in which the siderophore detection is spatially separated from the growth area of the bacterium.[26,27] The distinctive color change from blue to orange that can be observed in the presence of siderophores is often used to guide the isolation of these compounds after cultivation in a liquid medium. In case of *C. necator* H16, however, this methodology was not applicable,

dx.doi.org/10.1021/ja300620z | J. Am. Chem. Soc. 2012, 134, 5415−5422

since the required growth medium gave a false positive response in the liquid CAS assay, possibly due to an interference of media components.[27] We therefore set out to identify the potential siderophores from strain H16 by comparative metabolic profiling of cultures grown in the presence or absence of exogenous Fe(III), according to a previously established protocol.[28] While no additional peak (with significant signal intensity) showed up in the UV chromatogram of the iron-deficient culture, liquid chromatography electrospray ionization mass spectrometry (LC-ESI-MS) revealed the presence of distinctive pseudomolecular ions at m/z 808 $[M + H]^+$ and m/z 806 $[M - H]^-$, respectively. These ions disappeared once the culture was supplemented with 190 μM of $Fe(NH_4)$ citrate. To probe whether the annotated *cuc* cluster is involved in the biosynthesis of a putative siderophore with the corresponding mass, we disrupted the NRPS gene *cucH* by insertional mutagenesis (Figure S21, Supporting Information). The ensuing mutant strain was no longer capable to induce a color change in the modified CAS agar assay. Furthermore, it lacked the target ions at m/z 808 $[M + H]^+$ and m/z 806 $[M - H]^-$ when grown under iron limitation, thus confirming the involvement of *cucH* in siderophore assembly. The observation that the *cucH* mutant sustained its growth at low iron conditions suggests the presence of an alternative mechanism for iron acquisition. In compliance with the modified CAS assay, we did not detect any evidence for the production of vibrioferrin or another complementing siderophore by LC-MS and ^{1}H NMR analysis. We noticed, however, that *C. necator* H16 possesses an operon on chromosome 2, which encodes a ferrous iron uptake system (H16_B0083–H16_B0085).[29] The latter might, in conjunction with secreted Fe(III) reductases,[30,31] safeguard the iron supply of the bacterium.

For the isolation of the siderophore that derives from the *cuc* gene cluster, we evaluated different extraction conditions. The recovery of the water-soluble metabolite, which we tentatively named cupriachelin, was significantly increased by adsorption onto XAD-2 resin and subsequent elution with methanol. This approach did not only give a yield (6.5 mg/L) sufficient for UV detection but also revealed some minor metabolites in the same mass range, co-occurring with cupriachelin (Figure 2). Cleanup of cupriachelin was accomplished via reversed-phase chromatography.

Planar Structure and Complexing Properties of Cupriachelin. The empirical formula of cupriachelin was assigned to be $C_{33}H_{57}O_{16}N_7$ by high-resolution (HR)-ESI-MS (Figure S11, Supporting Information), which corresponds to 9 degrees of unsaturation. An inspection of the ^{13}C NMR spectrum immediately revealed that all double-bond equivalents could be ascribed to carbonyl moieties, five of which were present as amides according to heteronuclear long-range correlations with exchangeable protons at 8.65, 8.37, 8.33, 8.20, and 8.15 ppm. First-order multiplet analysis of the ^{1}H NMR spectrum and correlation spectroscopy (COSY) data allowed the discrimination of seven spin systems, including a decanoyl, a 3-hydroxybutanoyl, and five amino acid moieties (Figure S2, Supporting Information), which is consistent with the number of NRPS modules encoded on the *cuc* gene cluster. The preceding bioinformatic analyses facilitated the spectroscopic identification of the amino acid residues. As expected from the preliminary annotation of CucL and CucM, a discrete set of signals could be assigned to an N^{δ}-hydroxyornithine residue. HMBC interactions revealed that the latter was N-acylated with the 3-hydroxybutanoyl moiety, giving rise to a hydroxamate function. In accordance with the A domain specificity analysis, a glycine moiety could be deduced, while the two predicted Asp residues turned out to be β-hydroxylated in cupriachelin. The remaining amino acid, for which no prediction was available, could be identified as 2,4-diaminobutyric acid (Dab). The sequence of the single residues was finally determined exploiting NOE and HMBC correlations of the amide protons. The ensuing structure was subsequently confirmed by matrix-assisted laser desorption ionization time-of-flight (MALDI-TOF)/TOF fragmentation (Figure S2, Supporting Information).

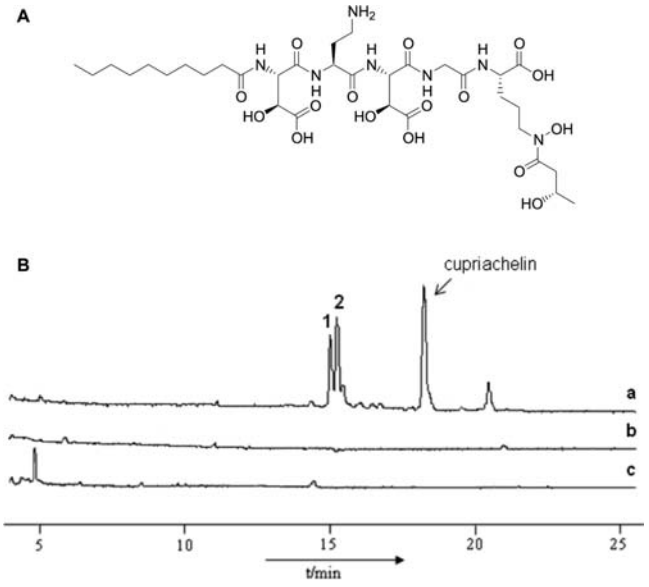

Figure 2. (A) Structure of cupriachelin. The stereochemistry was assigned following chemical derivatization of a cupriachelin acid hydrolysate by Marfey's method and chiral GC-MS, respectively. (B) Metabolic profiles of the *C. necator* H16 wild-type (profile a) and the *cucH* mutant strain (profile b) grown under iron-deficient conditions as well as from the wild-type strain in the presence of 190 μM $Fe(NH_4)$ citrate (profile c). The chemical structures of the metabolites (**1**) and (**2**) are given in Figure S1, Supporting Information.

During the structure elucidation of cupriachelin, we tested its preference for the coordination of different metal ions. MS studies showed that the natural product is forming monomeric 1:1 complexes with Fe^{3+} and Ga^{3+} (Figure S12, Supporting Information) but does not chelate Mn^{2+}, Co^{2+}, Ni^{2+}, Cu^{2+}, and Zn^{2+} (data not shown). The observed discrimination between divalent and trivalent cations, together with the Fe(III)-responsive production of cupriachelin, corroborates a potential siderophore role.

Absolute Configuration of Cupriachelin. To resolve the configuration of the amino acids in cupriachelin, we applied Marfey's method.[32] Acidic cleavage using 6 N HCl is a common strategy to liberate the amino acid constituents from a peptide and is usually successful when the latter is composed of proteinogenic amino acids only. In the case of cupriachelin, HCl-promoted hydrolysis yielded Dab, but the masses of the other amino acids could not be detected in the hydrolysate. To release the two β-hydroxyaspartic acid residues as well as the Orn moiety, a reductive HI cleavage was hence carried out.[33] Following the derivatization with Marfey's reagent (1-fluoro-2,4-dinitrophenyl-5-L-alanine amide, L-FDAA), the Dab and Orn residues of cupriachelin were both determined to be in L

dx.doi.org/10.1021/ja300620z | J. Am. Chem. Soc. 2012, 134, 5415–5422

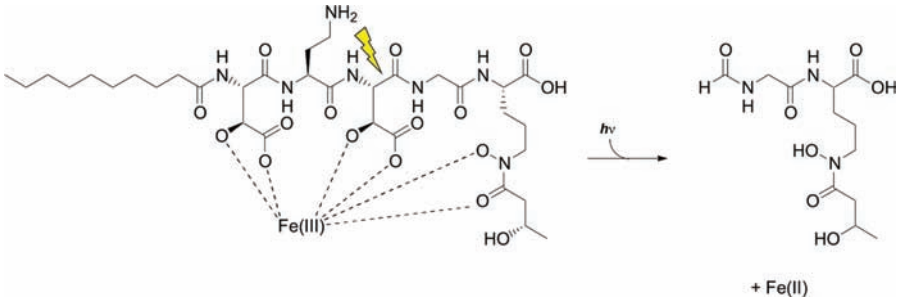

Figure 3. Proposed reaction scheme for the UV photolysis of Fe(III)-cupriachelin. The 'thunderbolt' indicates the position of cleavage. The depicted cleavage product was detected by HR-ESI-MS, and its structure was deduced by tandem mass spectrometry. Fe(III) is likely to be reduced via ligand-to-metal charge transfer.

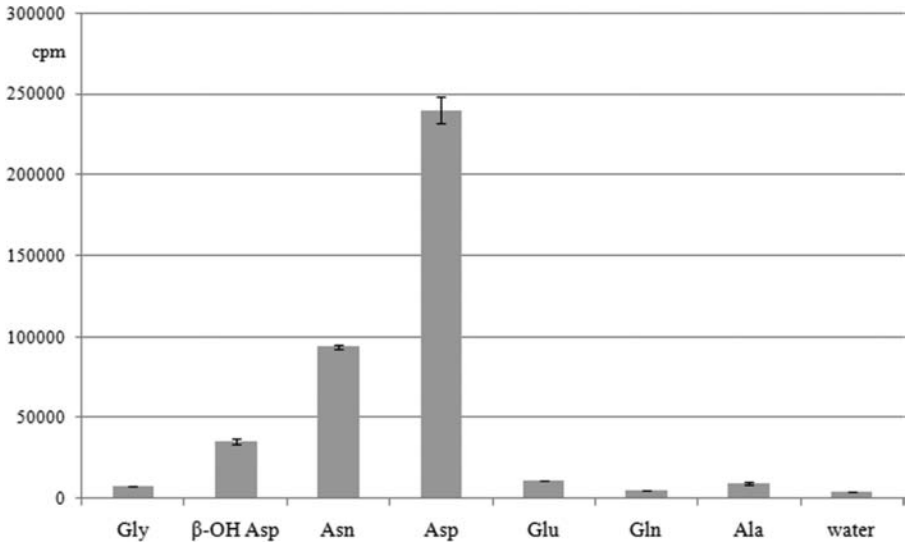

Figure 4. Relative activity of CucG with selected amino acids as judged by the ATP/PP_i exchange assay for adenylation function.

configuration (Figures S15 and S16, Supporting Information) . Furthermore, Marfey's method indicated the exclusive presence of *threo*-β-hydroxyaspartic acid in cupriachelin. It has previously been demonstrated that the elution order of the diastereomeric pairs of L-FDAA-derivatized *threo*-β-hydroxyaspartic acid is D→L under reversed-phase conditions.[34] The cupriachelin hydrolysate contained only one single peak of the correct mass upon conversion with L-FDAA, which was found to elute at the same retention time as the second peak of commercial D,L-*threo*-β-hydroxyaspartic acid (Figure S16, Supporting Information). This substantiates that, out of the four possible stereoisomers of β-hydroxyaspartic acid, only the L-*threo* form is present in cupriachelin.

To determine the configuration of the 3-hydroxybutyric acid (Hbu) moiety, we conducted a chiral separation on a GC column. Since the treatment of cupriachelin with neither concentrated HI nor 6 N HCl yielded intact Hbu, we resorted to a mild hydrolysis using 0.3 N HCl for 4 days at room temperature.[35] Upon conversion to its trifluoroacetyl ester, we identified L-Hbu by comparison with authentic standards (Figures S17 and S18, Supporting Information), thus establishing the complete stereochemistry of cupriachelin.

Photoreactivity of Cupriachelin. Cupriachelin exhibits structural features that are generally associated with siderophores from marine bacteria, including a fatty acid moiety and α-hydroxy acid residues, namely two β-hydroxyaspartates.[2,36] The latter were previously shown to mediate photolysis when coordinated to Fe(III), resulting in the reduction of the chelated ferric iron.[37] This redox cycling appears to have important ecological implications in the oceans. By releasing photoreactive siderophores, marine bacteria promote algal assimilation of iron and thus boost algal growth.[38] In return, they expand their pool of accessible organic carbon.[38] To evaluate whether cupriachelin is likewise prone to photochemical reactions, we exposed an aqueous solution of its ferric-ion complex to sunlight and analyzed the reaction via HR-ESI-MS (Figures S19 and S20, Supporting Information). As expected on the basis of its molecular structure, photolytic cleavage occurred at a β-hydroxyaspartate residue (Figure 3). The concomitant reduction of Fe(III) to Fe(II) was demonstrated in a second assay by trapping the latter with the specific chelating agent bathophenanthrolinedisulfonate (BPDS). Samples of Fe(III)-cupriachelin that were exposed to sunlight gradually turned red in the presence of BPDS, whereas light-protected control reactions stayed colorless in the same period. In the former case, the absorption at 535 nm increased from 0.002 ± 0.001 (prior to exposure) to 0.078 ± 0.002 (after exposure). The reactions that were kept in the dark showed a mean absorption of 0.006 ± 0.002 after the incubation, starting from absorption values of 0.005 ± 0.003. The absorbance of the ferrous tris(BPDS) complex was stable at room temperature for at least six hours.

CucG ATP/PP_i Exchange Assay. Considering the role of β-hydroxyaspartate in the photoreactivity of cupriachelin and

dx.doi.org/10.1021/ja300620z | J. Am. Chem. Soc. 2012, 134, 5415−5422

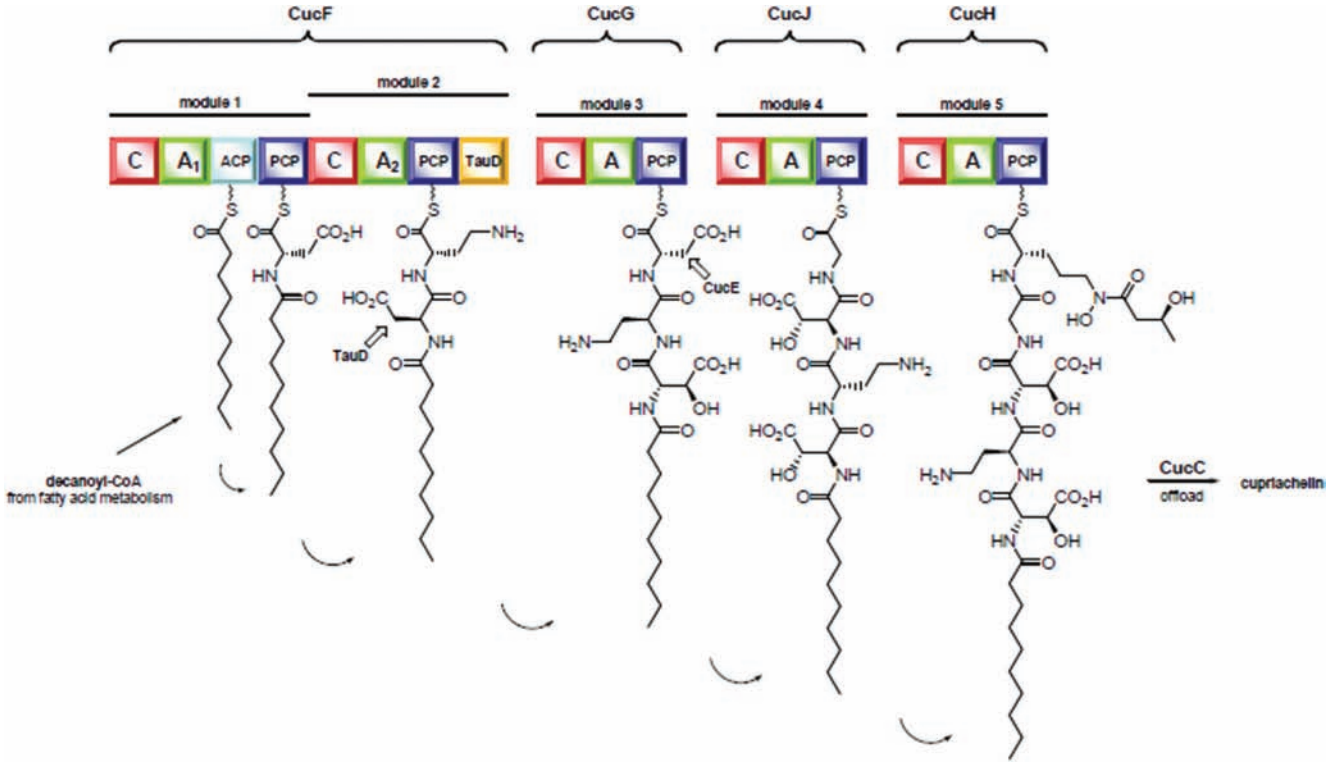

Figure 5. Proposed biosynthetic pathway for cupriachelin assembly. Domain notation: C, condensation; A, adenylation; ACP, acyl carrier protein; PCP, peptidyl carrier protein; and TauD, hydroxylase.

many other siderophores,[36] we were interested whether the formation of this nonproteinogenic amino acid occurs prior to the tethering to the assembly line or at a later biosynthetic stage. Both the manual and the computational specificity prediction of the responsible A domains (CucF-A_1 and CucG-A) suggested a preference for L-Asp (Table 1). On the other hand, a signature motif for β-hydroxyaspartate has not been reported to date. Therefore, we overexpressed and purified CucG from *Escherichia coli* BL21(DE3) as an N-terminal His-tag fusion via the expression plasmid pET28a(+) (Figure S22, Supporting Information). Biochemical characterization of the recombinant protein in the ATP/PP_i exchange assay revealed a distinct preference for Asp, confirming the bioinformatic prediction.[24,25] The results also showed affinity toward asparagine and β-hydroxyaspartate, albeit at significantly reduced levels, with the former being a somewhat better amino acid substrate than the latter (Figure 4). Despite intensive screening of *C. necator* H16, we did not find any evidence for the production of a cupriachelin derivative harboring an Asn residue. This suggests that the observed activity with Asn and β-hydroxyaspartate in the ATP/PP_i exchange assay is likely to be negligible.

Model for the Biosynthesis of Cupriachelin-Type Siderophores. Based upon the aforementioned bioinformatic and experimental results, a model for cupriachelin biosynthesis was deduced (Figure 5). Decanoic acid is hence proposed to act as the biosynthetic starter unit, but it can also be replaced by other fatty acids, e.g. octanoic acid or 3-hydroxydecanoic acid, as seen in some byproducts of the major metabolite cupriachelin (Figure S1, Supporting Information). Decanoic acid is expected to originate from fatty acid metabolism, where it is already present in its activated form as decanoyl-CoA or as its biosynthetic predecessor β-hydroxydecanoyl-CoA, respectively. Similar to the lipoinitiation reaction in surfactin biosynthesis,[39] the fatty acyl-CoA thioester is supposedly loaded onto the acyl carrier protein domain of module 1 and then transferred to the N-terminal C domain of CucF, which catalyzes the acylation of PCP-bound L-Asp. In the next two steps, the C domain of module 2 attaches the L-Dab moiety, and CucG (representing module 3) incorporates the following L-Asp residue. From the structure of cupriachelin it is clear that the CucJ-catalyzed condensation of Gly must precede the attachment of L-N^{δ}-hydroxy-N^{δ}-(3-hydroxybutyryl)-ornithine, which is carried out by the C domain of CucH. The fully assembled pentapeptidyl thioester is eventually released upon action of CucC.

Although the biosynthesis largely follows the classical NRPS enzymatic logic (maybe except for the sequence of reactions catalyzed by CucH and CucJ), the structure of cupriachelin could hardly be predicted from the analysis of its gene cluster due to the high fraction of functionalized, nonproteinogenic amino acids. By analyzing the substrate specificity of CucG, we have demonstrated that the hydroxylation of Asp must takes place after the initiating adenylation step, and we assume the same to be true for the CucF-derived Asp moiety. The discrete dioxygenase CucE as well as the C-terminal TauD domain of CucF are possible candidates to catalyze the required hydroxylations, which probably occur with the Asp residues tethered as protein-bound *S*-pantetheinyl thioesters, as shown in syringomycin biosynthesis.[40] In contrast, the preparation of L-Dab likely takes place prior to its adenylation, considering the specificity-determining amino acid residues in CucF-A_2. The aminotransferase CucA might be involved in the conversion of L-Asn to L-Dab, but this still needs to be proven. While the presence of an N-hydroxylated and N-acylated ornithine or lysine moiety was somewhat expected due to the annotation of

dx.doi.org/10.1021/ja300620z | J. Am. Chem. Soc. 2012, 134, 5415−5422

CucL and CucM, none of the A domains in the cupriachelin NRPS enzymes exhibited a motif indicating the priming of L-N^{δ}-formyl-N^{δ}-hydroxyornithine[10] or L-N^{δ}-acetyl-N^{δ}-hydroxyornithine.[12,41] As evidenced by the literature, the actually observed L-N^{δ}-hydroxy-N^{δ}-(3-hydroxybutyryl)-ornithine is not an uncommon constituent of siderophores,[2] but A domains that are responsible for the tethering of this amino acid have not been dissected to date.

In summary, we isolated and structurally characterized a new lipopeptide siderophore, cupriachelin, from the bioplastic producer *C. necator* H16. The secondary metabolite was discovered by using a genome mining strategy and represents the first natural product from the genus *Cupriavidus*. The ferric form of cupriachelin was shown to degrade when exposed to sunlight. At the same time, the coordinated Fe(III) is reduced, and ferrous iron is released, paralleling observations that have been made with siderophores from oceanic bacteria.[36] It is evident that a biological role for cupriachelin's photoreactivity is hardly imaginable in a soil environment. Yet, while most representatives of the species *Cupriavidus necator* are pertained to soil,[42] the investigated strain H16 was originally isolated from sludge of a creek.[43] The natural occurrence of the bacterium in a riverine habitat suggests a function for cupriachelin in freshwater ecology that is analogous to that of marine siderophores, i.e., supplying ferrous iron for uptake by planktonic assemblages.[37,38] The evolutionary destined release of the siderophore in an aquatic environment would also provide a plausible explanation for its amphiphilic structure. We assume that the inherent surface activity of cupriachelin will slow its diffusion away from the producing bacterium and secure a relatively high concentration around the cell.[44] Comparative genomics lends support toward our hypothesis on the biological role of cupriachelin: The majority of genes of *C. necator* H16 have orthologs in the genome of *C. necator* strain N-1,[45] but notwithstanding the great degree of global synteny between the two genomes, the *cuc* gene cluster is completely absent in the soil-derived N-1 strain.

EXPERIMENTAL PROCEDURES

Sequence Analyses. The genome of *C. necator* H16 consists of three circular replicons (GenBank accession numbers: NC_008313, NC_008314, and NC_005241, respectively), which were screened for genes putatively involved in siderophore biosynthesis using homology-based alignments. To identify potential biosynthetic gene clusters, initial hits were grouped by physical proximity and mapped onto the genome using Vector NTI (Invitrogen). Identified loci were further analyzed using Web-based bioinformatic software, e.g., NRPSpredictor2.[25]

General Experimental Procedures. LC-MS experiments were conducted on an Agilent 1100 series HPLC-DAD system coupled with an MSD trap (Agilent) operating in alternating ionization mode and an Antek 8060 HPLC-CLN detector (Antek Instruments GmbH) using a C8 column (Zorbax Eclipse XDB C8, 150 × 4.6 mm, 5 μm; Agilent). A linear gradient of methanol in water + 0.1% trifluoracetic acid (10% → 90% methanol within 15 min; flow rate 1 mL min^{-1}) was used for metabolic profiling. Analytical HPLC for Marfey's analysis was conducted on a Shimadzu UFLC liquid chromatography system equipped with a Nucleosil 100 C18 column (250 × 4.6 mm, 5 μm; CS Chromatographie service). The separation was accomplished by using a linear gradient from solvent A (10% acetonitrile in 25 mM aqueous KH_2PO_4) to solvent B (50% acetonitrile + 0.05% trifluoroacetic acid) over 40 min with wavelength monitoring at 365 nm. High-resolution mass determination was carried out using an Exactive Mass Spectrometer (Thermo-Scientific). NMR spectra were recorded at 300 K on a Bruker Avance III 500 MHz spectrometer with D_2O or H_2O/D_2O (4:1) as solvent and internal standard.

Bacterial Strains and Growth Conditions. *C. necator* H16 was grown in H-3 mineral medium lacking ammonium ferric citrate (1 g/L aspartic acid, 2.3 g/L KH_2PO_4, 2.57 g/L Na_2HPO_4, 1 g/L NH_4Cl, 0.5 g/L $MgSO_4 \times 7\ H_2O$, 0.5 g/L $NaHCO_3$, 0.01 g/L $CaCl_2 \times 2\ H_2O$, and 5 mL/L SL-6 trace element solution).[46] The influence of Fe^{3+} on cupriachelin production was tested in the same medium containing 190 μM ammonium ferric citrate. *E. coli* strains were cultured in liquid or solidified LB medium. When required, antibiotics were added to the following concentrations: 100 μg/mL ampicillin, 25 μg/mL chloramphenicol, and 50 μg/mL kanamycin, respectively.

Siderophore Screening. Chrome azurol S (CAS) plates were prepared as previously reported.[26,27] Half of each CAS agar layer was cut out, and the gap was filled with H-3 mineral medium agar. *C. necator* wild-type and mutant strains were plated on the H-3 half of the plates. The secretion of iron-scavenging molecules was detected by a color change from blue to orange after overnight incubation at 30 °C.

Construction of the *cucH* Disruption Mutant. A fragment of the gene-disruption target *cucH* was amplified by PCR from *C. necator* H16 genomic DNA with the primers P1 (5′-GAATTCAAGGGGCTGCGCGTTACGTC-3′) and P2 (5′-GAATTCACTGGTTGAAGCGGTTGCGGC-3′). The PCR product was cloned into pJET1.2 (Fermentas) to give pHiK003, which was subsequently transformed into *E. coli* BW25113/pIJ790 by electroporation.[47] Insertion of a kanamycin resistance cassette into the 2.2 kb gene fragment of *cchH* was achieved by λ red-mediated recombination.[47] For this purpose, sequences homologous to *cchH* were appended at either end of the resistance gene by PCR using primers P3 (5′-CCCGAACACGATGCCGAAATTGCCGTGCACCCGGCGCAGTGACTAACTAGGAGGAATAA-3′) and P4 (5′-AAACGGATCGGGAATAAAGCGGTCTGCCGTCATGCCGGCTATTCCTTCCAGTACTAAAC-3′) as well as pAphA-3 as the PCR template.[48] After the induction of λ red genes in *E. coli* BW25113/pIJ790/pHiK003 by addition of 10 mM L-arabinose at 30 °C, the cells were electrotransformed with the PCR product. Integration of the marker in the plasmid DNA by homologous recombination yielded the *cucH* disruption vector pHiK004. The latter was introduced into *C. necator* H16 by electroporation. For electroporation, the wild type of *C. necator* H16 was cultured in LB medium at 30 °C to an optical density of 0.4 at 600 nm. After centrifugation, the cells were washed with ice-cold washing buffer containing 1 mM *N*-(2-hydroxyethyl)-piperazine-*N*′-ethanesulfonic acid (pH 6.8) and 10% glycerol. The ensuing electrocompetent cells were transformed with pHiK004 in a 0.2 cm gap cuvette using a Bio-Rad GenePulser II set to 200 Ω, 25 μF, and 2.5 kV. SOC medium was added to the shocked cells, which were then cultured at 30 °C for 3 h. The regenerated culture was spread onto LB agar containing 350 μg/mL of kanamycin and incubated at 30 °C. Positive transformants were identified by colony PCR.

Isolation and Purification of Cupriachelin. *C. necator* H16 was cultivated in 5 L Erlenmeyer flasks filled with 2.5 L of H-3 mineral medium. The strain was shaken (150 rpm) at 30 °C for 3 days. At the end of cultivation, the culture supernatant was separated from the cells by centrifugation at 9500 × g and extracted with 150 g/L Amberlite XAD-2 (Supelco) for 24 h. After two washing steps with distilled water, the adsorbed metabolites were eluted from the resin with methanol. The ensuing eluate was concentrated under vacuum to dryness prior to resuspension in 1 mL of H_2O. Initial fractionation of the extract was accomplished by flash column chromatography over Polygoprep 60−50 C18 (Macherey-Nagel) using an increasing concentration of methanol in water. Fractions that showed the target ion at m/z 808 $[M + H]^+$ were further purified on a Shimadzu UFLC liquid chromatography system equipped with a Nucleodur C18 HTec column (VP 250 × 10 mm, 5 μm; Macherey-Nagel) using an isocratic flow of 30% acetonitrile in water + 0.1% trifluoroacetic acid at a flow rate of 4 mL min^{-1} with wavelength monitoring at 210 nm.

Amino Acid Analysis by Marfey's Method. Configuration of the amino acids present in cupriachelin was determined following acid hydrolysis and derivatization with Marfey's reagent[32] (1-fluoro-2,4-dinitrophenyl-5-L-alanine amide, L-FDAA, Sigma-Aldrich) by coelution

experiments with FDAA-derivatized amino acids. To this end, 500 μg purified cupriachelin was dissolved in 400 μL concentrated HI and heated at 110 °C for 3 h. The solution was lyophilized, and the dried hydrolysate was resuspended in 10 μL of water and 20 μL of 1 M $NaHCO_3$. Derivatization was carried out with 170 μL of 1% L-FDAA in acetone at 37 °C for 1 h. The products were lyophilized and prepared for LC-MS analysis by dissolving in 1 mL of 50% acetonitrile. Standards for cochromatography were prepared by reacting 50 μL of 50 mM aqueous amino acid solution with 20 μL of 1 M $NaHCO_3$ and 100 μL of 1% L-FDAA in acetone at 37 °C for 1 h. The lyophilized products were then dissolved in 1 mL of 50% acetonitrile. LC-MS analysis was performed under the aforementioned conditions with a detection wavelength of 365 nm. For the analysis of 2,4-diaminobutyric acid, we applied the traditional cleavage method with 6 N HCl for 24 h. The derivatization with L-FDAA was conducted as described for the HI cleavage products.

Configuration of the 3-Hydroxybutyrate Moiety. A 1 mL aliquot of 0.3 N HCl was added to 1.3 mg of cupriachelin in an Eppendorf vial. The vial was kept at room temperature for 4 days after which excess reagent was removed under vacuum. The hydrolysate was resuspended in water and purified over a Sep-Pak RP-18 cartridge. Following the removal of the eluent, 100 μL of trifluoroacetic anhydride/methylene chloride (1:1, v/v) was added, and the mixture heated at 100 °C for 10 min. Excess reagents were removed with a stream of argon. Methylene chloride, 100 μL, was added, and the resulting trifluoroacetyl ester analyzed using a Trace GC Ultra (Thermo) coupled in parallel to an FID detector and a Polaris-Q ion trap mass detector (Thermo). Separation was established on a chiral silica column (25 m × 0.25 mm ID) coated with Chir-D-Val (Varian) using a continuous He gas flow of 1.5 mL min^{-1} and a temperature gradient from 40 to 200 °C at a rate of 5 °C min^{-1}. Co-chromatography of the derivatized cupriachelin hydrolysate was conducted against a derivatized Hbu standard in D-configuration as well as a mixture containing both enantiomers.

Photoreactivity Test of Cupriachelin: Identification of Degradation Products. A 2 mM solution of ferric cupriachelin in PBS buffer (pH 7.5) was prepared and exposed to natural sunlight for 6 h. An identical solution that was shielded from sunlight served as a negative control. After photoexposure, both samples were dried in vacuo. The samples were then taken up in 100 μL of 50% methanol and subjected to LC coupled with HR-MS analysis. For this purpose, an Accela UPLC-system (Thermo Scientific) equipped with a Betasil C18 column (2.1 × 150 mm, 3 μm; Thermo Scientific) and an Exactive mass spectrometer was used. HPLC conditions were as follows: 5% → 98% acetonitrile in water + 0.1% formic acid within 15 min; flow rate 250 μL min^{-1}.

Photoreactivity Test of Cupriachelin: BPDS assay. Reduction of the complexed ferric iron to ferrous iron was examined using a modified photolysis assay as described for vibrioferrin.[38] Each reaction contained 100 μM cupriachelin, 10 μM $FeCl_3$, and 40 μM of the ferrous trapping agent BPDS (Fluka) in PBS buffer (pH 7.5). The reactions were either exposed to sunlight or stored in the dark for 4 h. The formation of $Fe(BPDS)_3^{2+}$ was recorded before and after exposure to sunlight/darkness by measuring the absorption at 535 nm using a Genesys 10 UV spectrophotometer (Thermo). All reactions were run in duplicate.

Cloning, Expression, and Purification of CucG. The entire ORF of *cucG* including a 30 nt sequence downstream of its stop codon was amplified by PCR with primers P5 (5′-C ATATGCCTGAGCTG-CAGTCCGCCTG-3′) and P6 (5′-GTATCACGGTCAATGGA-TATCGGGGAG-3′). The PCR product was cloned into pJET1.2 to give pHiK005. After digestion with NheI and HindIII, the resulting fragment was cloned as an N-terminal His-tag fusion into pET28a(+) (Novagen). The resulting vector pHiK006 was transformed into *E. coli* BL21(DE3) as an expression host. The overexpression strain was grown at 37 °C in terrific broth (TB) containing 50 μg/mL kanamycin to an OD of 0.6 at 600 nm. To induce the protein expression, 1 mM of isopropyl 1-thio-β-D-galactopyranoside (IPTG) was added to the culture, which was afterward incubated at 16 °C for 20 h. After centrifugation the cell pellet was resuspended in lysis buffer (50 mM NaH_2PO_4, 300 mM NaCl, 10 mM imidazole, 20 mM β-mercaptoethanol, 10% glycerol) and subjected to sonication. The cell debris was subsequently removed by centrifugation, and the supernatant was loaded onto a Ni-NTA column. The recombinant protein was eluted using lysis buffer containing increasing concentrations of imidazole. Fractions that contained the His-tagged CucG were identified via sodium dodecyl sulfate polyacrylamide gel electrophoresis (SDS-PAGE), desalted with PD-10 columns (GE Healthcare), and concentrated using Amicon ultracentrifugation devices (Millipore). The identity of the purified protein was confirmed by MALDI-TOF MS.

ATP/PP_i Exchange Assay. The substrate preference of the adenylation domain of CucG was determined by amino acid-dependent exchange of the radiolabel from [^{32}P]-pyrophosphate (PP_i) to ATP according to established protocols.[49] A 100 μL reaction contained 80 mM Tris-HCl (pH 7.5), 5 mM $MgCl_2$, 5 mM ATP, 100 nM purified enzyme, 0.1 mM [^{32}P]-pyrophosphate, and 1 mM amino acid. Reactions were initiated by addition of enzyme and incubated at 37 °C for 30 min prior to quenching with 500 μL of charcoal suspension (1% charcoal and 4.5% $Na_4P_2O_7$ in 3.5% perchloric acid). Precipitate was collected with paper filter discs under vacuum. Following three consecutive washing steps with 40 mM $Na_4P_2O_7$ in 1.4% perchloric acid (200 mL), water (200 mL), and ethanol (200 mL), the filter papers were added to 2.5 mL of scintillation fluid and read by a Beckman Coulter LS6500 multipurpose scintillation counter. All reactions were run in triplicate.

■ ASSOCIATED CONTENT

Ⓢ Supporting Information

A complete annotation of the *cuc* gene cluster, including GenBank accession numbers, NMR data and spectra of cupriachelin, MS data of cupriachelin and its minor congeners, HPLC-MS and GC-MS of cupriachelin stereochemistry assignment, photoreactivity test of Fe(III)-cupriachelin, PCR-based confirmation of *cucH* gene disruption, and SDS-PAGE of purified recombinant CucG. This material is available free of charge via the Internet at http://pubs.acs.org.

■ AUTHOR INFORMATION

Corresponding Author

Markus.Nett@hki-jena.de.

Notes

The authors declare no competing financial interest.

■ ACKNOWLEDGMENTS

We gratefully acknowledge financial support from the Bundesministerium für Bildung und Forschung (BMBF GenoMik-Transfer programme; grant no. 0315591A) and from the Jena School for Microbial Communication (JSMC). We thank A. Perner and M. Poetsch (Hans-Knöll-Institute Jena) for numerous HR-ESI-MS and MALDI-TOF/TOF measurements, respectively. We are further indebted to D. Hoffmeister (Friedrich-Schiller-Universität Jena) and his research group for valuable discussions as well as advice on the experimental setup of the ATP/PP_i exchange assay. We also thank N. Überschaar (Hans-Knöll-Institute Jena, Department of Biomolecular Chemistry) for help with the GC analysis.

■ REFERENCES

(1) Andrews, S. C.; Robinson, A. K.; Rodriguez-Quinones, F. *FEMS Microbiol. Rev.* **2003**, *27*, 215−237.

(2) (a) Hider, R. C.; Kong, X. *Nat. Prod. Rep.* **2010**, *27*, 637−657. (b) Sandy, M.; Butler, A. *Chem. Rev.* **2009**, *109*, 4580−4595. (c) Miethke, M.; Marahiel, M. A. *Microbiol. Mol. Biol. Rev.* **2007**, *71*, 413−451.

(3) D'Onofrio, A.; Crawford, J. M.; Stewart, E. J.; Witt, K.; Gavrish, E.; Epstein, S.; Clardy, J.; Lewis, K. *Chem. Biol.* **2010**, *17*, 254−264.
(4) Paauw, A.; Leverstein-van Hall, M. A.; van Kessel, K. P. M; Verhoef, J.; Fluit, A. C. *PLoS ONE* **2009**, *4*, e8240.
(5) Walsh, C. T.; Liu, J.; Rusnak, R.; Sakaitani, M. *Chem. Rev.* **1990**, *90*, 1105−1129.
(6) de Lorenzo, V.; Bindereif, A.; Paw, B. H.; Neilands, J. B. *J. Bacteriol.* **1986**, *165*, 570−578.
(7) Crosa, J. H.; Walsh, C. T. *Microbiol. Mol. Biol. Rev.* **2002**, *66*, 223−249.
(8) Challis, G. L. *ChemBioChem* **2005**, *6*, 601−611.
(9) Fischbach, M. A.; Walsh, C. T. *Chem. Rev.* **2006**, *106*, 3468−3496.
(10) Lautru, S.; Deeth, R. J.; Bailey, L. M.; Challis, G. L. *Nature Chem. Biol.* **2005**, *1*, 265−269.
(11) Dimise, E. J.; Widboom, P. F.; Bruner, S. D. *Proc. Natl. Acad. Sci. U.S.A.* **2008**, *105*, 15311−15316.
(12) (a) Lazos, O.; Tosin, M.; Slusarczyk, A. L.; Boakes, S.; Cortes, J.; Sidebottom, P. J.; Leadlay, P. F. *Chem. Biol.* **2010**, *17*, 160−173. (b) Robbel, L.; Knappe, T. A.; Linne, U.; Xie, X.; Marahiel, M. A. *FEBS J.* **2010**, *277*, 663−676.
(13) Bosello, M.; Robbel, L.; Linne, U.; Xie, X.; Marahiel, M. A. *J. Am. Chem. Soc.* **2011**, *133*, 4587−4595.
(14) Seyedsayamdost, M. R.; Traxler, M. F.; Zheng, S.-L.; Kolter, R.; Clardy, J. *J. Am. Chem. Soc.* **2011**, *133*, 11434−11437.
(15) Nett, M.; Ikeda, H.; Moore, B. S. *Nat. Prod. Rep.* **2009**, *26*, 1362−1384.
(16) Winter, J. M.; Behnken, S.; Hertweck, C. *Curr. Opin. Chem. Biol.* **2011**, *15*, 22−31.
(17) Steinbüchel, A. *Macromol. Biosci.* **2001**, *1*, 1−24.
(18) Vincent, K. A.; Cracknell, J. A.; Lenz, O.; Zebger, I.; Friedrich, B.; Armstrong, F. A. *Proc. Natl. Acad. Sci. U.S.A.* **2005**, *102*, 16951−16954.
(19) Schwartz, E.; Henne, A.; Cramm, R.; Eitinger, T.; Friedrich, B.; Gottschalk, G. *J. Mol. Biol.* **2003**, *332*, 369−383.
(20) Pohlmann, A.; Fricke, W. F.; Reinecke, F.; Kusian, B.; Liesegang, H.; Cramm, R.; Eitinger, T.; Ewering, C.; Pötter, M.; Schwartz, E.; Strittmatter, A.; Voß, I.; Gottschalk, G.; Steinbüchel, A.; Friedrich, B.; Bowien, B. *Nat. Biotechnol.* **2006**, *24*, 1257−1262.
(21) Price, M. N.; Huang, K. H.; Alm, E. J.; Arkin, A. P. *Nucleic Acids Res.* **2005**, *33*, 880−892.
(22) Felnagle, E. A.; Barkei, J. J.; Park, H.; Podevels, A. M.; McMahon, M. D.; Drott, D. W.; Thomas, M. G. *Biochemistry* **2010**, *49*, 8815−8817.
(23) Rausch, C.; Hoof, I.; Weber, T.; Wohlleben, W.; Huson, D. H. *BMC Evol. Biol.* **2007**, *7*, 78.
(24) Stachelhaus, T.; Mootz, H. D.; Marahiel, M. A. *Chem. Biol.* **1999**, *6*, 493−505.
(25) Röttig, M.; Medema, M. H.; Blin, K.; Weber, T.; Rausch, C.; Kohlbacher, O. *Nucleic Acids Res.* **2011**, *39*, W362−W367.
(26) Milagres, A. M.; Machuca, A.; Napoleao, D. *J. Microbiol. Methods* **1999**, *37*, 1−6.
(27) Schwyn, B.; Neilands, J. B. *Anal. Biochem.* **1987**, *160*, 47−56.
(28) Kreutzer, M. F.; Kage, H.; Gebhardt, P.; Wackler, B.; Saluz, H. P.; Hoffmeister, D.; Nett, M. *Appl. Environ. Microbiol.* **2011**, *77*, 6117−6124.
(29) Cartron, M. L.; Maddocks, S.; Gillingham, P.; Craven, C. J.; Andrews, S. C. *BioMetals* **2006**, *19*, 143−157.
(30) Cowart, R. E. *Arch. Biochem. Biophys.* **2002**, *400*, 273−281.
(31) Schröder, I.; Johnson, E.; de Vries, S. *FEMS Microbiol. Rev.* **2003**, *27*, 427−447.
(32) Marfey, P. *Carlsberg Res. Commun.* **1984**, *49*, 591−596.
(33) Stephan, H.; Freund, S.; Meyer, J.-M.; Winkelmann, G.; Jung, G. *Liebigs Ann. Chem.* **1993**, 43−48.
(34) Fujii, K.; Ikai, Y.; Mayumi, T.; Oka, H.; Suzuki, M.; Harada, K. *Anal. Chem.* **1997**, *69*, 3346−3352.
(35) Schaffner, E. M.; Hartmann, R.; Taraz, K.; Budzikiewicz, H. *Z. Naturforsch., C* **1996**, *51*, 139−150.
(36) Butler, A.; Theisen, R. M. *Coord. Chem. Rev.* **2010**, *254*, 288−296.
(37) Barbeau, K.; Rue, E. L.; Bruland, K. W.; Butler, A. *Nature* **2001**, *413*, 409−413.
(38) Amin, S. A.; Green, D. H.; Hart, M. C.; Küpper, F. C.; Sunda, W. G.; Carrano, C. J. *Proc. Natl. Acad. Sci. U.S.A.* **2009**, *106*, 17071−17076.
(39) Kraas, F. I.; Helmetag, V.; Wittmann, M.; Strieker, M.; Marahiel, M. A. *Chem. Biol.* **2010**, *17*, 872−880.
(40) Singh, G. M.; Fortin, P. D.; Koglin, A.; Walsh, C. T. *Biochemistry* **2008**, *47*, 11310−11320.
(41) Schwecke, T.; Göttling, K.; Durek, P.; Duenas, I.; Käufer, N. F.; Zock-Emmenthal, S.; Staub, E.; Neuhof, T.; Dieckmann, R.; von Döhren, H. *ChemBioChem* **2006**, *7*, 612−622.
(42) Balkwill, D. L. In *Bergey's Manual of Systematic Bacteriology*, 2nd ed. Boone, D. R., Castenholz, R. W., Garrity, G. M., Brenner, D. J., Krieg, N. R., Staley, J. T., Eds.; Springer: New York, 2005; Vol. *2*, pp 600−604.
(43) Wilde, E. *Arch. Mikrobiol.* **1962**, *43*, 109−137.
(44) Martinez, J. S.; Carter-Franklin, J. N.; Mann, E. L.; Martin, J. D.; Haygood, M. G.; Butler, A. *Proc. Natl. Acad. Sci. U.S.A.* **2003**, *100*, 3754−3759.
(45) Poehlein, A.; Kusian, B.; Friedrich, B.; Daniel, R.; Bowien, B. *J. Bacteriol.* **2011**, *193*, 5017.
(46) Pfennig, N. *Arch. Microbiol.* **1974**, *100*, 197−206.
(47) Gust, B.; Challis, G. L.; Fowler, K.; Kieser, T.; Chater, K. F. *Proc. Natl. Acad. Sci. U.S.A.* **2003**, *100*, 1541−1546.
(48) Ménard, R.; Sansonetti, P. J.; Parsot, C. *J. Bacteriol.* **1993**, *175*, 5899−5906.
(49) Wackler, B.; Schneider, P.; Jacobs, J. M.; Pauly, J.; Allen, C.; Nett, M.; Hoffmeister, D. *Chem. Biol.* **2011**, *18*, 354−360.